Mineralogical Magazine (2022), **86**, 331–339
doi:10.1180/mgm.2022.26

CAMBRIDGE UNIVERSITY PRESS

Article

Tennantite-(Cu), $Cu_{12}As_4S_{13}$, from Layo, Arequipa Department, Peru: a new addition to the tetrahedrite-group minerals

Cristian Biagioni[1]*, Jiří Sejkora[2], Yves Moëlo[3], Eric Marcoux[4], Daniela Mauro[5] and Zdeněk Dolníček[2]

[1]Dipartimento di Scienze della Terra, Università di Pisa, Via Santa Maria 53, 56126 Pisa, Italy; [2]Department of Mineralogy and Petrology, National Museum, Cirkusová 1740, 193 00, Praha 9, Czech Republic; [3]Université de Nantes, CNRS, Institut des Matériaux Jean Rouxel, IMN, F-44000 Nantes, France; [4]ISTO – CNRS, Orléans University, 1A, rue de la Férollerie – CS 20066, F-45071 Orléans Cedex 2, France; and [5]Museo di Storia Naturale, Università di Pisa, Via Roma 79, 56011 Calci (PI), Italy

Abstract

Tennantite-(Cu), $Cu_{12}As_4S_{13}$, was approved as a new mineral species from the Layo epithermal deposit, Castilla Province, Arequipa Department, Peru, where it occurs as black metallic anhedral grains, up to 0.1 mm across, replacing enargite and associated with chalcopyrite and vinciennite. In reflected light, tennantite-(Cu) is isotropic, grey with a bluish shade. Reflectance data for the four COM wavelengths in air are [λ (nm): *R* (%)]: 470: 29.1; 546: 28.4; 589: 27.4; and 650: 25.0. Electron microprobe analysis for holotype material gave (in wt.% – average of 10 spot analyses): Cu 49.32(27), Fe 2.20(12), Zn 0.09(2), Sn 0.03(5), As 19.45(43), Sb 1.94(10), Te 0.02(5), S 27.75(43), total 100.80(20). On the basis of (As + Sb + Te) = 4 atoms per formula unit (apfu), the empirical formula of tennantite-(Cu) is $(Cu_{11.27}Fe_{0.57}Zn_{0.02})_{\Sigma 11.86}(As_{3.77}Sb_{0.23})_{\Sigma 4.00}S_{12.57}$. Tennantite-(Cu) is cubic, $I\bar{4}3m$, with unit-cell parameters $a = 10.1710(10)$ Å, $V = 1052.2(2)$ Å^3 and $Z = 2$. Its crystal structure was refined by single-crystal X-ray diffraction data to a final $R_1 = 0.0178$ on the basis of 263 unique reflections with $F_o > 4\sigma(F_o)$ and 24 refined parameters. Tennantite-(Cu) is isotypic with other tetrahedrite-group minerals. Previous findings of tennantite-(Cu) are reported and some nomenclature issues, related to the Fe and Cu oxidation states, are discussed. At the Layo epithermal deposit, tennantite-(Cu) is the result of the replacement of enargite under decreasing f_{S_2} conditions.

Keywords: tennantite-(Cu), new mineral, sulfosalt, copper, arsenic, crystal structure, Layo, Peru

(Received 15 February 2022; accepted 13 March 2022; Accepted Manuscript published online: 21 March 2022; Associate Editor: Daniel Atencio)

Introduction

Tetrahedrite-group minerals are characterised by the general structural formula $^{M(2)}A_6{}^{M(1)}(B_4C_2)^{X(3)}D_4{}^{S(1)}Y_{12}{}^{S(2)}Z$, where the capital letters indicate several chemical constituents. Among the different species, the most commons belong to the tetrahedrite and tennantite series and are characterised by A and B = Cu^+, D = Sb^{3+} or As^{3+}, and Y and Z = S^{2-}. Different C constituents, usually represented by divalent transition elements, identify the species belonging to these series (Biagioni *et al.*, 2020).

'Tennantite' was the first name of a mineral belonging to the tetrahedrite group to be introduced by the brothers Richard and William Phillips (R. Phillips, 1819; W. Phillips, 1819) and it honours the English chemist Smithson Tennant (1761–1815). The material studied, from Cornwall, England, was Fe-rich. Later, 'zincian tennantite' was reported from some localities (e.g. Freiberg, Saxony, Germany – Plattner, 1846; Lengenbach, Binn Valley, Switzerland – Des Cloizeaux, 1855; Miedzianka, Świętokrzyskie Voivodeship, Poland – Morozewicz, 1926). Biagioni *et al.* (2020) renamed these species as tennantite-(Fe) and tennantite-(Zn). Iron and Zn are the most common divalent elements occurring in tennantite-series minerals; moreover, since the publication of the nomenclature of tetrahedrite-group minerals (Biagioni *et al.*, 2020), three other species belonging to the tennantite series have been approved by the International Mineralogical Association – Commission on New Minerals, Nomenclature and Classification (IMA-CNMNC), i.e. tennantite-(Hg) (Biagioni *et al.*, 2021), tennantite-(Ni) (Wang *et al.*, 2021), and tennantite-(Cd) (Biagioni *et al.*, 2022). Other potential end-member compositions are known in the literature. Among them, compositions corresponding to ideal $Cu_{12}As_4S_{13}$ have been reported, for instance, from Canada, France and Peru (Johan and Le Bel, 1980; Thouvenin, 1983; Cesbron *et al.*, 1985; Marcoux *et al.*, 1994).

The re-examination of a specimen from the Peruvian epithermal deposit of Layo (Marcoux *et al.*, 1994) allowed the description of the new mineral species tennantite-(Cu). The new mineral and its name (symbol Tnt-Cu) have been approved by the Commission on New Minerals, Nomenclature and Classification of the International Mineralogical Association (IMA-CNMNC), under the voting number 2020-096. Part of holotype material of tennantite-(Cu) is deposited in the collections of the Department of Mineralogy and Petrology, National Museum in Prague, Cirkusová 1740, 193 00 Praha 9, Czech Republic under the catalogue number P1P 74/2020, in the collections of the Museo di Storia Naturale of the Università di Pisa, Via Roma

*Author for correspondence: Cristian Biagioni, Email: cristian.biagioni@unipi.it
Cite this article: Biagioni C., Sejkora J., Moëlo Y., Marcoux E., Mauro D. and Dolníček Z. (2022) Tennantite-(Cu), $Cu_{12}As_4S_{13}$, from Layo, Arequipa Department, Peru: a new addition to the tetrahedrite-group minerals. *Mineralogical Magazine* **86**, 331–339. https://doi.org/10.1180/mgm.2022.26

79, Calci (PI), under catalogue number 19925, and in the collections of the Mineralogical Museum of Ecole des Mines de Paris (MINES ParisTech) under catalogue number ENSMP 83990.

In this paper the description of this new species belonging to the tetrahedrite group is reported and some crystal-chemical and nomenclature issues are discussed.

Occurrence and physical properties

Tennantite-(Cu), described initially as 'Cu-excess tennantite' by Marcoux *et al.* (1994), was found in the Layo epithermal deposit (15°11'16"S, 72°14'30"W), Castilla Province, Arequipa Department, Peru (Fig. 1). The Layo vein system is formed by anastomosing veins hosted in NNE–SSW-striking fractures in Miocene–Pliocene volcanic rocks belonging to the Tazaca Group. This rock sequence is formed by two distinct successions: the first one is a 300 m thick sequence of ignimbritic lava flows and pyroclastic tuffs, dacitic to rhyolitic in compositions (Pisaca Formation), whereas the second one, known as the Jullujia Formation, is composed by discordant andesitic lava flows and domes, as well as by pyroclastic rocks. In the Layo area, the volcanic rocks are affected by a pervasive propylitic alteration. Around ore vein systems, propylitised rocks occur as relicts within hydrothermally altered silicic-argillic zones. Marcoux *et al.* (1994) gave further details about the geological background of the Layo epithermal deposit.

Tennantite-(Cu) was collected in the eastern zone of the ore field, in the so-called Vetas 7 and 8. In these veins, a breccia, formed by silicified and alunitised angular rock clasts, is cemented by an ore assemblage composed of complex Cu–As–Fe–Sn sulfides, showing banded and cockade textures related to the rhythmic alternation of pyrite and Cu–As–Sn sulfides, i.e. enargite, tennantite-(Cu), chalcopyrite and vinciennite (Marcoux *et al.*, 1994). The mineralogy is dominated by early pyrite succeeded by a late complex Cu–As–Sn association where tennantite-(Cu) is the prominent sulfide (Fig. 2). Tennantite-(Cu) is associated with enargite, chalcopyrite and vinciennite, that often form ameboid oriented patches up to 80 μm in size, sometimes developed from relicts of enargite. Secondary minerals also formed, such as bornite, covellite and digenite, at the expense of chalcopyrite, and scarce luzonite at the expense of enargite.

Tennantite-(Cu) is black in colour, with a black streak and metallic lustre. Mohs hardness was not measured, owing to the small size of the grain studied and the intimate association of other sulfides, but it should be close to 3½–4, in agreement with other members of the tetrahedrite group. Tennantite-(Cu) is brittle, with a conchoidal fracture and an indistinct cleavage. Due to the small size of the grains studied and their admixture with other sulfides, density was not measured; on the basis of the empirical formula and the single-crystal X-ray diffraction data, the calculated density is 4.656 g·cm^{-3}.

In reflected light, tennantite-(Cu) is isotropic. It is grey, with a bluish shade (Fig. 2). Internal reflections were not observed. Reflectance values measured in air on the holotype sample using a spectrophotometer MSP400 Tidas at Leica microscope, with a 50× objective, are given in Table 1 and shown in Fig. 3, where the reflectance curve for tennantite-(Cu) is compared with published data for other tetrahedrite-group minerals.

Chemical data

Quantitative chemical analyses were carried out using a Cameca SX 100 electron microprobe (National Museum of Prague, Czech Republic) and the following experimental conditions: wavelength dispersive spectroscopy mode, accelerating voltage = 25 kV and beam current = 20 nA, beam diameter = 1 μm. Standards (element, emission line) were: chalcopyrite (Cu*K*α and S*K*α), pyrite (Fe*K*α), ZnS (Zn*K*α), NiAs (As*L*β), Sn (Sn*L*α), Sb_2S_3 (Sb*L*α) and PbTe (Te*M*α). The contents of other sought elements with $Z > 8$ (Ag, Au, Bi, Cd, Co, Ga, Ge, Hg, In, Mn, Cl, Ni, Pb, Se and Tl) were below detection limits. Matrix correction by the PAP procedure (Pouchou and Pichoir, 1985) was applied to the data. Electron back-scattered images showed that tennantite-(Cu) is slightly zoned, with a domain richer in Sb, 30–40 μm in size, located on the margin of the grain. Results are given in Table 2.

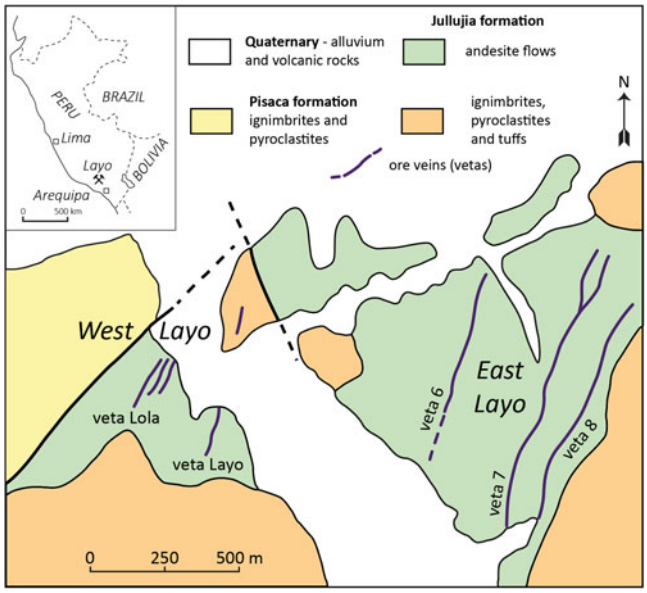

Fig. 1. The Layo ore district: location and geology (simplified after Marcoux *et al.*, 1994).

X-ray crystallography

Single-crystal X-ray diffraction intensity data were collected on an anhedral grain of tennantite-(Cu), 60 μm × 40 μm × 30 μm in size, using a Bruker Apex II diffractometer (50 kV and 30 mA) equipped with a Photon II CCD detector and graphite-monochromatised Mo*K*α radiation (Dipartimento di Scienze della Terra, Università di Pisa, Italy). The detector-to-crystal distance was set at 50 mm. Data were collected using φ scan mode in 0.5° slices, with an exposure time of 30 s per frame, and they were corrected for Lorentz, polarisation, absorption and background effects using the software package *Apex*3 (Bruker AXS Inc., 2016). The refined unit-cell parameters are $a = 10.1710(10)$ Å, $V = 1052.2(2)$ Å^3; and space group $I\bar{4}3m$. The crystal structure of tennantite-(Cu) was refined using *Shelxl-2018* (Sheldrick, 2015) starting from the structural model of Johnson and Burnham (1985). The following neutral scattering curves, taken from the *International Tables for Crystallography* (Wilson, 1992) were used initially: Cu *vs* □ at *M*(2), Cu *vs* Fe at *M*(1), As *vs* Sb at *X*(3), S at S(1) and S(2) sites.

Several cycles of isotropic refinement converged to $R_1 = 0.115$, confirming the correctness of the structural model. The modelling of the racemic twin suggested that the structure had to be inverted.

https://doi.org/10.1180/mgm.2022.26 Published online by Cambridge University Press

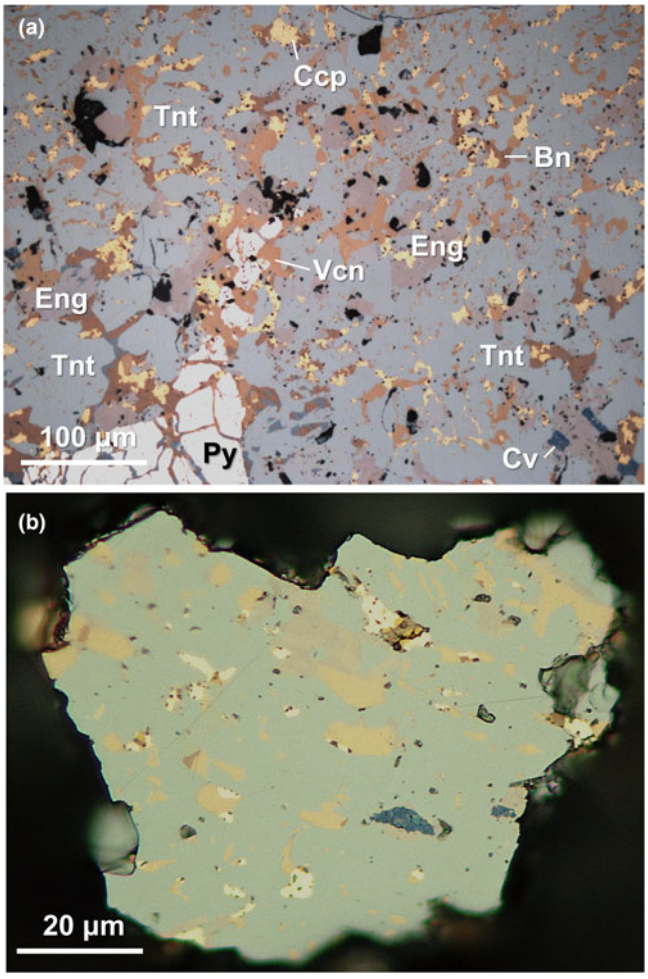

Fig. 2. (a) Association of tennantite-(Cu) (Tnt, bluish grey), with pyrite (Py, yellowish white), chalcopyrite (Ccp, yellow), enargite (Eng, purplish pale grey), vinciennite (Vcn, orange-brown) and secondary Cu sulfides: bornite (Bn, brown) and covellite (Cv, blue). Veta 8, Layo epithermal deposit. Reflected light microscope (plane polarised light). Mineral symbols after Warr (2021). (b) Holotype material of tennantite-(Cu), associated with the same phases shown in (a), as seen in reflected light microscopy (partly crossed polars). Catalogue number P1P 74/2020.

An anisotropic refinement for cations only converged to $R_1 = 0.0280$. The relatively large U_{eq} value of the $M(2)$ site suggested its split nature, in agreement with previous authors (Andreasen *et al.*, 2008; Welch *et al.*, 2018). After the addition of the split position, found in the difference-Fourier map, the R_1 value was lowered to 0.0210. The site occupancy factors (s.o.f.) at the two split positions $M(2a)$ and $M(2b)$ were constrained to be 1, as no Cu excess at the $M(2)$ site was detected. After several cycles of anisotropic refinement for all the atoms, the R_1 converged to 0.0178 for 263 unique reflections with $F_o > 4\sigma(F_o)$ and 24 refined parameters. Details of the data collection and crystal structure refinement are reported in Table 3. Fractional atomic coordinates and equivalent isotropic displacement parameters are reported in Table 4, whereas Table 5 reports selected bond distances and Table 6 the weighted bond-valence sums (BVS) calculated according to the bond parameters of Brese and O'Keeffe (1991). The crystallographic information file has been deposited with the Principal Editor of *Mineralogical Magazine* and is available as Supplementary material (see below).

Powder X-ray diffraction data were not collected, owing to the small size of the available grains and admixture with other phases (in particular, vinciennite). Table 7 reports the calculated X-ray powder diffraction pattern.

Table 1. Reflectance data for tennantite-(Cu).*

λ (nm)	*R* (%)	λ (nm)	*R* (%)
400	30.7	560	28.2
420	30.4	580	27.7
440	30.0	**589**	**27.4**
460	29.3	600	27.0
470	**29.1**	620	26.2
480	28.9	640	25.4
500	28.7	**650**	**25.0**
520	28.6	660	24.6
540	28.4	680	23.9
546	**28.4**	700	23.4

*The reference wavelengths required by the Commission on Ore Mineralogy (COM) are given in bold.

Results and discussions

Chemical formula

As discussed in previous papers (e.g. Sejkora *et al.*, 2021), there are different approaches to recalculate the chemical formulae of tetrahedrite-group minerals. The two better ones normalise the number of atoms on the basis of $\Sigma Me = 16$ atoms per formula unit (apfu) or on the basis of (As + Sb + Te + Bi) = 4 apfu. The former approach assumes that no vacancies occur at the $M(2)$, $M(1)$, and $X(3)$ sites, whereas the latter is based mainly on the results discussed by Johnson *et al.* (1986) who revealed that negligible variations in the ideal number of $X(3)$ atoms usually occur.

The first approach gives the chemical formula $Cu_{11.36(10)}Fe_{0.58(3)}Zn_{0.02(1)}(As_{3.80(7)}Sb_{0.23(1)})_{\Sigma 4.03}S_{12.67(24)}$, whereas the other normalisation strategy corresponds to the formula $Cu_{11.27(31)}Fe_{0.57(3)}Zn_{0.02(1)}(As_{3.77(1)}Sb_{0.23(1)})_{\Sigma 4.00}S_{12.57(47)}$. These formulae are in agreement with previous results of Marcoux *et al.* (1994). Their average formula, recalculated on the basis of $\Sigma Me = 16$ apfu, taking into account the average formula given in their Table 3, is $Cu_{11.37}Fe_{0.66}Zn_{0.02}(As_{3.74}Sb_{0.21})_{\Sigma 3.95}S_{13.51}$. Copper, Fe and Zn contents agree with those found in this work, as well as the As/(As+Sb) atomic ratios.

The simplified formula of tennantite-(Cu) is $Cu_6Cu_4(Cu,Fe,Zn)_2(As,Sb)_4S_{13}$, corresponding to the end-member formula $Cu_6^+(Cu_4^+Cu_2^{2+})As_4S_{13}$. It corresponds to (in wt.%) Cu 51.56, As 20.26, S 28.18, total 100.00.

The Sb-enriched domain corresponds to the chemical formula (based on $\Sigma Me = 16$ apfu) $Cu_{11.35(2)}Fe_{0.65(1)}Zn_{0.03(1)}(As_{2.78(4)}Sb_{1.10(2)}Te_{0.09(1)})_{\Sigma 3.97}S_{12.85(8)}$. This domain is characterised by a distinctly higher Sb content [Sb/(As+Sb+Te) atomic ratio passing from 0.06 to 0.28] and detectable Te content.

Crystal structure description

Tennantite-(Cu) is isotypic with the other members of the tetrahedrite group. Its crystal structure (Fig. 4) can be described as a framework of corner-sharing $M(1)S(1)_4$ tetrahedra with cages hosting $X(3)S(1)_3$ trigonal pyramids around $S(2)M(2)_6$ octahedra (*e.g.* Johnson *et al.*, 1988).

The tetrahedrally coordinated $M(1)$ site is a mixed (Cu,Fe) site, with only minor amounts of Zn. The refined site scattering is 171.48 electrons per formula unit (epfu), to be compared with the value calculated from the site population proposed on the

https://doi.org/10.1180/mgm.2022.26 Published online by Cambridge University Press

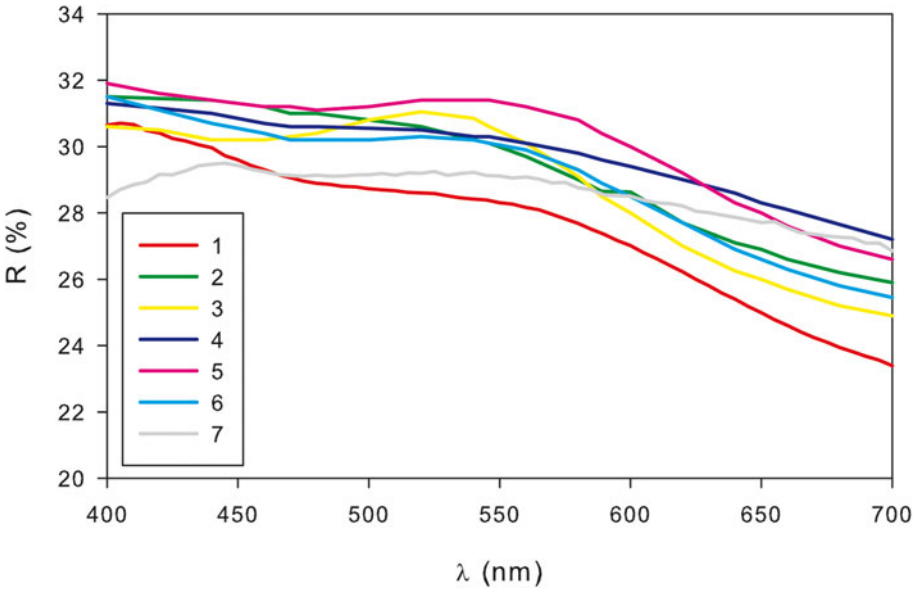

Fig. 3. Reflectance curves for tennantite-(Cu) from the Layo deposit, compared with published data for other tennantite-series minerals. (1) Layo, Arequipa Department, Peru; (2) tennantite-(Fe) from Wheal Jewel, Cornwall, England (Criddle and Stanley, 1993; p. 557); (3) tennantite-(Zn) from Tsumeb, Otavi, Namibia (Criddle and Stanley, 1993; p. 561); (4) Bi-bearing tennantite-(Zn) from the Bicknoller Quarry, Cornwall, England (Criddle and Stanley, 1993; p. 558); (5) Hg-bearing tennantite-(Fe) from the Gortdrum mine, Ireland (Criddle and Stanley, 1993; p. 559); (6) Pb-bearing tennantite-(Zn) from the Sark's Hope mine, Sark, Channel Islands (Criddle and Stanley, 1993; p. 560); and (7) tennantite-(Hg) from Lengenbach, Switzerland (Biagioni *et al.*, 2021).

basis of electron microprobe data, $^{M(1)}(Cu_{5.40}Fe_{0.58}Zn_{0.02})$, i.e. 172.26 epfu. Average bond distance is 2.3075 Å. The BVS at the *M*(1) site, 1.36 valence units (vu), agrees with a site with Cu^{+} mixed with higher valency cations.

The *M*(2) site is split into two sub-positions, *M*(2a) and *M*(2b), separated by 0.60 Å, whereas the distance between two neighbouring *M*(2b) positions is 1.20 Å. These distances are shorter than those observed in Cu-rich unsubstituted tennantite described by Makovicky *et al.* (2005), having *M*(2a)–*M*(2b) and *M*(2b)–*M*(2b) distances of 1.08 and 2.00 Å, respectively. The *M*(2a) position has a triangular planar coordination, whereas *M*(2b) has a flat trigonal pyramidal one. This feature agrees with previous studies (e.g. Andreasen *et al.*, 2008; Welch *et al.*, 2018). Average bond distances are 2.230 and 2.307 Å for *M*(2a) and *M*(2b) positions, respectively. Such values can be compared with those reported in Cu-pure and unsplit *M*(2) sites occurring in tetrahedrite and tennantite studied by Wuensch (1964) and Wuensch *et al.* (1966), respectively, i.e. 2.259 and 2.240 Å, respectively, as well as with those reported by Makovicky *et al.* (2005), i.e. 2.217 Å for Cu2A and 2.467 Å for Cu2B. The Cu2B of Makovicky *et al.* (2005) is also close to the As site, 2.41 Å, whereas the *M*(2b)–*X*(3) distance is 2.835 Å in the sample from Layo. In this latter sample, copper was the only cation at the *M*(2) site, in agreement with electron microprobe data. The larger size of the *M*(2b) position is probably due to its average nature. During the refinement of tennantite-(Cu) from Layo, an unconstrained refinement of the s.o.f. at the *M*(2a) and *M*(2b) sites was performed, resulting in $M(2a) = Cu_{0.650(19)}$ and $M(2b) = Cu_{0.162(9)}$, with a site population at *M*(2) corresponding to $^{M(2)}Cu_{5.84}$, not suggesting any Cu excess. For this reason, as described above, the sum of the s.o.f. at *M*(2a) and *M*(2b) was constrained to be 1. On the contrary, Makovicky *et al.* (2005) found a slight Cu excess, with a surplus of ca. 10%. The BVS at the *M*(2) site [i.e. *M*(2a) + 2×*M*(2b)] (Table 6) is 1.04 valence units (vu), in agreement with the presence of monovalent cations.

The splitting of the *M*(2) position is variable in the tetrahedrite–tennantite sub-group. In Fe-bearing compounds synthesised at 450°C (Fe between ~ 0.3 and 2 apfu), Andreasen *et al.* (2008) only found a split (24*g*) site. A single-crystal synchrotron X-ray diffraction study of synthetic $Cu_{12}Sb_4S_{13}$ and $Cu_{12}As_4S_{13}$ was performed recently by Hathwar *et al.* (2019) from room temperature down to 70 K. Whereas in synthetic $Cu_{12}Sb_4S_{13}$ there is only a single (12*e*) site (but with a high atomic displacement perpendicular to the triangle) the use of high resolution data allowed the resolution of the *M*(2) site of synthetic $Cu_{12}As_4S_{13}$ into six (24*g*) sub-positions.

The *X*(3) site shows an average bond distance of 2.266 Å. Taking into account the electron microprobe data, the site occupancy $(As_{0.95}Sb_{0.05})$ can be proposed. It corresponds to a mean atomic number of 33.90 electrons, to be compared with the refined mean atomic number of 34.03 electrons. Assuming idealised *X*–S distances of 2.26 and 2.45 Å for As^{3+} and Sb^{3+}, respectively (calculated according to the bond parameters of Brese and O'Keeffe, 1991), an average *X*(3)–S(1) distance of 2.270 Å can be expected. The BVS is 3.06 vu.

The S(1) site is four-fold coordinated and is bonded to two *M*(1), one *M*(2) [i.e. *M*(2a) or one of the two mutually-exclusive *M*(2b)] and one *X*(3). Its BVS is 2.04 vu. S(2) is octahedrally coordinated by atoms hosted at *M*(2) sites, with a BVS of 2.16 vu. Both S sites were found fully occupied.

Coupling the results of the crystal structure refinement and the electron microprobe analysis, the structural formula of holotype tennantite-(Cu) can be written as $^{M(2)}Cu_{6.00}{}^{M(1)}(Cu_{5.40}Fe_{0.58}Zn_{0.02})^{X(3)}(As_{0.95}Sb_{0.05})_4S_{13}$.

Relation between unit-cell parameter and chemical composition

Unit-cell parameter of tennantite-(Cu) from Layo (i.e. $a = 10.171$ Å) agrees with that of synthetic sample No. 2052 of Makovicky *et al.* (2003), having composition $Cu_{11.24}Fe_{0.57}As_{3.93}S_{13.00}$ and unit-cell parameter $a = 10.174(8)$ Å. The 'Cu-rich unsubstituted tennantite' of Makovicky *et al.* (2005) has $a = 10.1756(9)$ Å. Applying the relationships between chemistry and unit-cell parameter proposed by Johnson *et al.* (1987), to the sample from Layo one obtains a value of 10.22 Å; a better fit is obtained using the relations proposed by Charlat and Lévy (1975), i.e. 10.19 Å.

https://doi.org/10.1180/mgm.2022.26 Published online by Cambridge University Press

Table 2. Chemical data for tennantite-(Cu) and Sb-rich tennantite-(Cu).

	Tennantite-(Cu) (n = 10)			Sb-rich tennantite-(Cu) (n = 4)		
Element	wt.%	range	e.s.d.	wt.%	range	e.s.d.
Cu	49.32	48.80–49.66	0.27	47.40	47.33–47.48	0.07
Fe	2.20	2.00–2.26	0.12	2.40	2.34–2.43	0.04
Zn	0.09	0.06–0.11	0.02	0.12	0.10–0.14	0.02
Sn	0.03	0.00–0.15	0.05	-	-	-
As	19.45	18.98–20.25	0.43	13.71	13.59–13.94	0.16
Sb	1.94	1.78–2.05	0.10	8.84	8.67–8.99	0.17
Te	0.02	0.00–0.17	0.05	0.73	0.62–0.89	0.12
S	27.75	26.84–28.30	0.43	27.10	26.99–27.23	0.11
Total	100.80	100.32–101.00	0.20	100.28	100.08–100.52	0.22

n = number of spot analyses.

Several recent studies on synthetic Fe-free $Cu_{12}As_4S_{13}$ gave the following unit-cell parameter a = 10.163(7) Å (Levinsky *et al.*, 2019), with composition actually $Cu_{11.81}As_{4.19}S_{12.67}$, based on ΣMe = 16 apfu; a = 10.1572(2) Å at 293 K (Yaroslavzev *et al.*, 2021); and a = 10.1554(6) Å at 300 K (Hathwar *et al.*, 2019).

Comparison between tennantite-(Cu) and previous findings of Cu-rich tennantite

Natural members of the tennantite series are usually characterised by the formula $Cu_6(Cu_4Me_2)As_4S_{13}$, where *Me* is commonly Fe and Zn. However, synthetic $Cu_{12}As_4S_{13}$ has been synthesised, in some cases showing a Cu excess with respect to the ideal 12 apfu. For instance, Maske and Skinner (1971) studied the system Cu–As–S and found a compositional field $Cu_{12+x}As_{4+y}S_{13}$, with $0 < x < 1.72$ and $0 < y < 0.08$. Unit-cell variation from 10.168 to 10.222 Å was reported for compositions $\sim Cu_{12}As_4S_{13}$ and $\sim Cu_{14}As_4S_{13}$, respectively. Lind and Makovicky (1982) highlighted an analytical problem during electron microprobe analysis of synthetic tetrahedrite-group phases; indeed, those compositions having Cu > 12 apfu gave the same analytical results as those having 12 Cu apfu. This effect was noted for both Sb- and As-members of this sulfosalt group.

In literature, the term 'Cu-excess' was first used by Marcoux *et al.* (1994) to indicate a Cu content higher than 10 apfu. According to the work of Lind and Makovicky (1982) and Makovicky *et al.* (2005), this term ought to be reserved to compounds with Cu over 12 apfu. Some of these Cu-rich tennantite-series minerals (Cu > 10 apfu) correspond to what is now classified as tennantite-(Cu), whereas others are simply Cu-rich varieties of tennantite-(Fe). For instance, sample M14 of Charlat and Lévy (1974), from Trevisane, Cornwall, England, having a chemical formula $Cu_{10.70}Fe_{1.27}Zn_{0.03}As_{3.97}S_{12.90}$, may be labelled as tennantite-(Fe), as its formula can be recast as $Cu_6[Cu_4(Fe_{1.27}Cu_{0.70}Zn_{0.03})]As_{3.97}S_{12.90}$. On the contrary, samples from Huaron, Peru (Thouvenin, 1983), Chizeuil, France (Cesbron *et al.*, 1985) and Lornex, Canada (Johan and Le Bel, 1980) correspond to tennantite-(Cu); at the French locality, a potential tetrahedrite-(Cu) was also reported.

Other findings of tennantite-(Cu) were reported by Kouzmanov *et al.* (2004) from the Radka deposit, Bulgaria. The samples studied by these authors show Cu contents ranging from 10.88 to 11.26 apfu, Fe between 0.79 and 1.14 apfu, and Zn below the detection limit. The observed As/(As+Sb+Bi) atomic ratio is in the range 0.90–0.98. Ideally, samples from this locality correspond to the formula $Cu_{11}Fe(As_{3.8}Sb_{0.2})S_{13}$.

Table 3. Summary of crystal data and parameters describing data collection and refinement for tennantite-(Cu).

Crystal data	
Crystal size (mm)	0.060 × 0.040 × 0.030
Cell setting, space group	Cubic, $I\bar{4}3m$
a (Å)	10.1710(10)
V (Å^3)	1052.2(2)
Z	2
Data collection	
Radiation, wavelength (Å)	Mo$K\alpha$, λ = 0.71073
Temperature (K)	293(2)
$2\theta_{max}$ (°)	57.58
Measured reflections	1693
Unique reflections	279
Reflections with $F_o > 4\sigma(F_o)$	263
R_{int}	0.0296
$R\sigma$	0.0301
Range of h, k, l	$-12 \le h \le 12$, $-13 \le k \le 5$, $-11 \le l \le 11$
Refinement	
R [$F_o > 4\sigma(F_o)$]	0.0178
R (all data)	0.0202
wR (on F_o^2)[1]	0.0375
Goof	0.968
Absolute structure parameter[2]	0.03(3)
Number of least-squares parameters	24
Maximum and minimum residual peak (e^- Å^{-3})	0.27 [at 1.01 Å from X(3)] −0.28 [at 0.90 Å from M(2b)]

[1] $w = 1/[\sigma^2(F_o^2)+1.3875P]$.
[2] Flack (1983)

Catchpole *et al.* (2012) reported chemical data of tetrahedrite-group minerals from the Morococha base metal district, Peru. Chemical compositions vary between tetrahedrite-(Zn) in the Ag–Pb zone to tennantite-(Zn) in the Zn–Pb–Ag and Zn–Cu zones, and to tennantite-(Cu) in the Cu zone. Actually, in this last zone Cu varies between 11.10 and 11.60 apfu, and Fe is the second most abundant C constituent (ranging from 0.44 to 0.70 apfu), with low contents of Zn (from below the detection limit to 0.23 apfu). The As/(As+Sb+Te) atomic ratio ranges between 0.59 and 0.88.

Repstock *et al.* (2015) described Cu-rich tennantite from the Pefka mine, Greece; at this locality, tennantite-(Cu) shows As/(As+Sb+Te) atomic ratios ranging between 0.73 and 0.94 (also samples with Sb > As were observed) and Fe/(Fe+Zn+Hg) varying between 0.01 and 0.75, i.e. from nearly Fe-free samples, with Zn as the second most abundant C constituent, to Fe-rich phases.

Velebil *et al.* (2021) described Zn-free tennantite samples from Julcani ore district, Peru, with 0.61–0.94 Fe apfu and Sb only up to 0.09 apfu which also correspond to tennantite-(Cu).

Finally, Voudouris *et al.* (2022) reported an interesting In- and Cu-rich tennantite from the Pefka mine, Greece. This occurrence deserves further discussion below.

Notwithstanding these previous occurrences of tennantite-(Cu), the first structural characterisation of a pure Cu-tennantite-series mineral was reported by Makovicky *et al.* (2005) using a sample from Cerro Atajo Cu–Au deposit, in the Province of Catamarca, Argentina. Its chemical formula, based on (As + Sb) = 4 apfu, is $Cu_{12.5}(As_{3.92}Sb_{0.08})S_{12.4}$. Makovicky *et al.* (2005) found ~10% excess of Cu, with s.o.f. at the split M(2a) and M(2b) sites of $Cu_{0.75(2)}$ and $Cu_{0.17(1)}$, resulting in a site population at M(2) corresponding to $^{M(2)}Cu_{6.54}$. As discussed above, such a Cu excess was not found in the sample from Layo.

https://doi.org/10.1180/mgm.2022.26 Published online by Cambridge University Press

Table 4. Sites, Wyckoff positions, site occupancy factors (s.o.f.), fractional atom coordinates and equivalent isotropic displacement parameters (Å^2) for tennantite-(Cu).

Site	Wyckoff position	s.o.f.	*x/a*	*y/b*	*z/c*	U_{eq}
M(2)	12*e*	$Cu_{0.669(18)}$	0.7830(2)	0	0	0.034(2)
M(2b)	24g	$Cu_{0.166(9)}$	0.7814(6)	0.0417(8)	–0.0417(8)	0.034(2)
M(1)	12*d*	$Cu_{0.86(4)}Fe_{0.14(4)}$	¾	½	0	0.0195(4)
X(3)	8*c*	$As_{0.947(11)}Sb_{0.053(11)}$	0.73827(6)	0.73827(6)	0.73827(6)	0.0158(3)
S(1)	24*g*	$S_{1.00}$	0.88030(12)	0.88030(12)	0.64200(15)	0.0151(4)
S(2)	2*a*	$S_{1.00}$	0	0	0	0.0221(10)

Table 5. Selected bond distances (Å) for tennantite-(Cu).

M(1)–S(1)	×4	2.3075(10)	*M*(2b)–S(2)		2.302(7)
			M(2b)–S(1)	×2	2.310(4)
M(2a)–S(2)		2.207(3)			
M(2a)–S(1)	×2	2.2410(19)	*X*(3)–S(1)	×3	2.2655(15)

Table 6. Weighted bond-valence sums (in valence unit) for tennantite-(Cu).*

Site	*M*(1)	*M*(2a)	*M*(2b)	*X*(3)	Σanions	Theor.
S(1)	$^{2\times\rightarrow}0.34^{\times4\downarrow}$	$0.24^{\times2\downarrow}$	$^{2\times\rightarrow}0.05^{\times2\downarrow}$	$1.02^{\times3\downarrow}$	2.04	2.00
S(2)		$^{6\times\rightarrow}0.26$	$^{12\times\rightarrow}0.05$		2.16	2.00
Σcations	1.36	0.74	0.15	3.06		
Theor.	1.33	0.67	0.17	3.00		

*Note: left and right superscripts indicate the number of equivalent bonds involving cations and anions, respectively. The following site populations were used: *M*(2a) = $Cu_{0.669}$; *M*(2b) = $Cu_{0.166}$; *M*(1) = $Cu_{0.900}Fe_{0.097}Zn_{0.003}$; *X*(3) = $As_{0.95}Sb_{0.05}$.

Table 7. X-ray powder diffraction data for tennantite-(Cu).*

I_{calc}	d_{calc}	*h k l*	I_{calc}	d_{calc}	*h k l*
1	7.192	1 1 0	1	1.995	5 1 0
4	4.152	2 1 1	4	1.995	4 3 1
2	3.596	2 2 0	**8**	**1.857**	**5 2 1**
1	3.216	3 1 0	**43**	**1.798**	**4 4 0**
100	**2.936**	**2 2 2**	2	1.744	4 3 3
3	2.718	3 2 1	1	1.650	5 3 2
18	**2.543**	**4 0 0**	4	1.650	6 1 1
3	2.397	3 3 0	1	1.608	6 2 0
3	2.397	4 1 1	**21**	**1.533**	**6 2 2**
1	2.168	3 3 2	2	1.468	4 4 4
1	2.076	4 2 2	1	1.438	7 1 0

*Intensity and d_{hkl} were calculated using the software *PowderCell2.4* (Kraus and Nolze, 1996) on the basis of the structural model given in Table 4. Only reflections with I_{calc} > 1 are listed. The five strongest reflections are given in bold.

Nomenclature issues in Cu-rich tennantite

Type material of tennantite-(Cu) has a chemical composition close to $Cu_{11.4}Fe_{0.6}(As_{3.75}Sb_{0.25})S_{13} = {}^{A}Cu_6[{}^{B}Cu_{4.0}{}^{C}(Cu_{1.4}Fe_{0.6})]{}^{D}(As_{3.75}Sb_{0.25})S_{13}$. Following Biagioni *et al.* (2020), this chemistry can be idealised to the end-member formula $Cu^{+}_{10}Cu^{2+}_{2}As_4S_{13}$, assuming that formally divalent Cu^{2+} is the most abundant C constituent. However, in agreement with the results of Mössbauer studies performed by Makovicky *et al.* (2003) on synthetic Fe-bearing tennantite, the most probable composition of the sample studied from Layo could be $^{A}Cu_6[^{B}Cu_{4.0}C(Cu^{2+}_{0.8}Cu^{+}_{0.6}Fe^{3+}_{0.6})]^{D}(As_{3.75}Sb_{0.25})S_{13}$. Indeed, sample 2052 of Makovicky *et al.* (2003), with chemical formula $Cu_{11.24}Fe_{0.57}As_{3.93}S_{13}$ (similar to that of the natural Peruvian specimen), showed Fe^{3+} as the dominant iron species. If so, applying the site-total-charge approach (Bosi *et al.*, 2019), the end-member formula $Cu_6(Cu^{+}_5Fe^{3+})As_4S_{13} = Cu_{11}Fe^{3+}As_4S_{13}$ is achieved. This result is in agreement with the hypothesis of Marcoux *et al.* (1994) about the presence of Fe^{3+} in the specimen from Layo, due to the high f_{S_2}.

It is worth noting that a virtually Fe-free or Fe-poor tennantite-(Cu) is reported by Repstock *et al.* (2015). Analyses 4 and 10 of these authors (see their table 3) correspond (on the basis of $\Sigma Me = 16$ apfu) to $Cu_{10.99}Ag_{0.01}(Zn_{0.89}Fe_{0.01})(As_{3.00}Sb_{1.03}Te_{0.07})(S_{12.97}Se_{0.01})$ and $Cu_{11.14}(Zn_{0.79}Fe_{0.09})(As_{2.33}Sb_{1.66})S_{13.54}$, whereas analyses 7 and 8 have compositions $Cu_{11.68}Ag_{0.01}(Fe_{0.18}Zn_{0.08})(As_{3.80}Sb_{0.25})S_{13.22}$ and $Cu_{11.62}(Fe_{0.29}Zn_{0.09})(As_{3.76}Sb_{0.24})S_{13.42}$, respectively. The two former analyses have a possible site population at *M*(1) corresponding to $^{M(1)}[Cu_{4.00}(Cu_{1.10}Zn_{0.89}Fe_{0.01})]$ and $^{M(1)}[Cu_{4.00}(Cu_{1.12}Zn_{0.79}Fe_{0.09})]$, with the C constituent represented by formally divalent Cu (Zn is the second most abundant C constituent). The remaining two analyses show Cu^{2+} as the dominant C constituent, even considering Fe as Fe^{3+}: $^{M(1)}[Cu_{4.00}(Cu^{2+}_{1.56}Cu^{+}_{0.18}Fe^{3+}_{0.18}Zn_{0.08})]$ and $^{M(1)}[Cu_{4.00}(Cu^{2+}_{1.33}Cu^{+}_{0.29}Fe^{3+}_{0.29}Zn_{0.09})]$. The end-member formula $Cu_6(Cu^{+}_4Cu^{2+}_2)As_4S_{13}$ can be applied to all these samples.

Thus, the solid solution from the Fe pole to the Cu pole would correspond ideally to the following sequence ('ionic' model): (1) $Cu^{+}_{10}Fe^{2+}_2$ → (2) $Cu^{+}_{10.5}Fe^{2+}Fe^{3+}_{0.5}$ → (3) $Cu^{+}_{11}Fe^{3+}$ → (4) $Cu^{+}_{10.5}Cu^{2+}Fe^{3+}_{0.5}$ → (5) $Cu^{+}_{10}Cu^{2+}_2$. Compositions (1) to (3) correspond to the substitution rule $2Fe^{2+} \rightarrow Cu^{+} + Fe^{3+}$, and compositions (3) to (5) to $Cu^{+} + Fe^{3+} \rightarrow 2Cu^{2+}$. This sequence, controlled by an increase of f_{S_2}, indicates that iron oxidation precludes the appearance of formally divalent copper. According to nomenclature rules, one ought to distinguish three species: (i) 'tennantite-(Fe^{2+})', from formula (1) up to formula (2), (ii) 'tennantite-(Fe^{3+})', from formula (2) up to formula (4), and (iii) 'tennantite-(Cu^{2+})', from formula (4) up to formula (5).

On this basis, composition of tennantite-(Cu) from the Layo epithermal deposit falls in the field of 'tennantite-(Fe^{3+})'. Nevertheless, studies of natural and synthetic samples of tetrahedrite-(Cu) and tennantite-(Cu) using various physical methods revealed a very complex crystal chemistry, not completely understood up to now. After initial examinations in the 1970s, the first detailed ^{57}Fe-Mössbauer studies were performed on Fe-bearing tetrahedrite in the 1990s (Charnock *et al.*, 1989; Makovicky *et al.*, 1990 and references herein) and completed by Nasonova *et al.* (2016) and Sobolev *et al.* (2017). Iron-bearing synthetic tennantite was studied by Makovicky *et al.* (2003). Though the first studies confirm major Fe^{2+} towards the Fe pole, and major Fe^{3+} towards the Cu pole, examination of tennantite indicates the presence of Fe^{2+} down to 0.5 Fe apfu, as well as mixed valence Fe. Mixed valence iron seems to represent a substantial fraction of total iron at room *T*, owing to charge-transfer phenomena between Cu and Fe. For instance, at

https://doi.org/10.1180/mgm.2022.26 Published online by Cambridge University Press

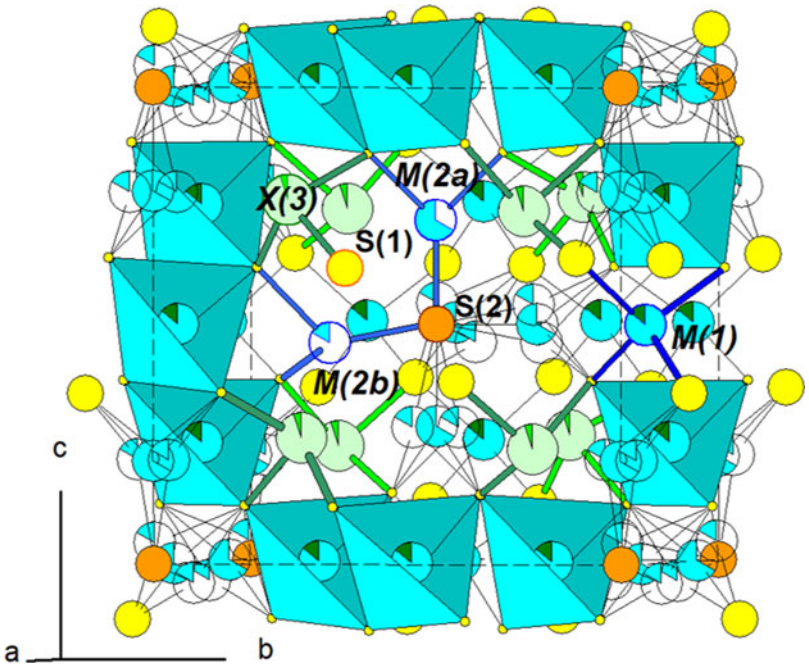

Fig. 4. Crystal structure of tennantite-(Cu). Several atoms in front of the unit cell have been suppressed, to enhance atom coordination. S (1): yellow; S(2): orange; *X*(3): green; *M*(1): blue (Cu) and dark green (Fe), with representation of some tetrahedra (blue); *M*(2a) and *M*(2b): blue (Cu) and white (vacancy).

a content of 0.5 Fe apfu, Makovicky *et al.* (2003) estimated a formal valence ranging between +2.68 and +2.69 (+2.68 for sample 2052). The oxidation state of Cu was determined by Pattrick *et al.* (1993) and Gainov *et al.* (2008) on natural tetrahedrite and tennantite, and by Di Benedetto *et al.* (2005) on synthetic $Cu_{12}Sb_4S_{13}$. These three studies revealed the presence of divalent Cu in all Cu-rich samples. Nevertheless, though Di Benedetto *et al.* (2005) proposed two Cu^{2+} apfu, located on the Cu1 site, Pattrick *et al.* (1993), confirmed by Gainov *et al.* (2008), indicates that Cu^{2+} located on the Cu2 triangular site, is sometimes present for compositions excluding it according to the ionic model. Moreover, in normal conditions, pure $Cu_{12}Sb_4S_{13}$ and $Cu_{12}Sb_4S_{13}$ are metallic (Lu and Morelli, 2013), which would correspond to partial replacement of Cu^{2+} by Cu^{+} and one ligand hole (i.e. mobile S electron).

It thus appears that in Cu-rich tetrahedrite/tennantite one may have coexistence of Fe^{3+}, Fe^{2+}, Cu^{2+} and Cu^{+} (with ligand hole). The distinction between three species envisaged above on the basis of a simple ionic model is not pertinent, and it is more convenient, for nomenclature purposes, to consider only two species, tennantite-(Fe) and tennantite-(Cu). The sample from Layo can thus be classified as tennantite-(Cu), as Cu is more abundant than Fe as the C constituent.

A special case is represented by In-bearing tennantite-series minerals reported by Voudouris *et al.* (2022) from Pefka, Greece. These samples show up to 0.893 In apfu, with 11.049 Cu apfu, thus corresponding to the end-member $Cu_6(Cu_5In^{3+})As_4S_{13}$. As no ambiguity in the oxidation state of In can be assumed, this phase should be regarded as different from tennantite-(Cu), and it may represent the new species 'tennantite-(In)'.

Genesis of tennantite-(Cu)

The ore assemblages where tennantite-(Cu) occurs are usually composed of enargite, $Cu_3As^{5+}S_4$, vinciennite, $Cu_7^{+}Cu_3^{2+}Fe_2^{2+}Fe_2^{3+}SnAs^{5+}S_{16}$, mawsonite, $Cu_6^{+}Fe_2^{3+}SnS_8$, and chalcopyrite, $Cu^{+}Fe^{3+}S_2$ (e.g. Chizeuil, France – Cesbron *et al.*, 1985; Layo, Peru – Marcoux *et al.*, 1994; Radka, Bulgaria – Kouzmanov *et al.*, 2004); these assemblages are typical of high-sulfidation conditions. Tennantite-(Cu) usually replaces enargite, probably as a consequence of decreasing f_{S_2} in the crystallisation environment, usually during the early stages of the evolution of epithermal systems. On the contrary, Makovicky *et al.* (2005) proposed that 'Cu-excess tennantite-(Cu)' from Catamarca, Argentina, was related to (Fe/Zn)-poor late-stage hydrothermal solutions. However, the samples show inclusions of luzonite, the low *T*-dimorph of enargite (Maske and Skinner, 1971), and watanabeite, ideally $Cu_4(As,Sb)_2^{5+}S_5$; thus, a genesis similar to those proposed for other occurrences cannot be discarded.

Conclusion

The description of tennantite-(Cu) adds further complexity to the tetrahedrite group, confirming on one side the structural plasticity of these chalcogenides, hosting several metals typical of hydrothermal settings, and on the other side their role in recording the crystallisation conditions of ore assemblages.

In addition to improving the knowledge of ore mineralogy, the description of this new phase gives further information about the crystal chemistry of tetrahedrite-group minerals, with possible technological implications, as revealed by several recent studies focusing on the thermoelectric properties of these compounds (e.g. Chetty *et al.*, 2015; Levinsky *et al.*, 2019).

Supplementary material. To view supplementary material for this article, please visit https://doi.org/10.1180/mgm.2022.26

Acknowledgements. CB acknowledges financial support from the Ministero dell'Istruzione, dell'Università e della Ricerca through the project PRIN 2017 "TEOREM – deciphering geological processes using Terrestrial and Extraterrestrial ORE Minerals", prot. 2017AK8C32. The study was also financially supported by the Ministry of Culture of the Czech Republic (long-term

project DKRVO 2019-2023/1.II.d; National Museum, 00023272) for JS and ZD. The comments of Peter Leverett and two anonymous reviewers improved the original manuscript.

References

Andreasen J.W., Makovicky E., Lebech B. and Karup-Møller S. (2008) The role of iron in tetrahedrite and tennantite determined by Rietveld refinement of neutron powder diffraction data. *Physics and Chemistry of Minerals*, **35**, 447–454.

Biagioni C., George L.L., Cook N.J., Makovicky E., Moëlo Y., Pasero M., Sejkora J., Stanley C.J., Welch M.D. and Bosi F. (2020) The tetrahedrite group: Nomenclature and classification. *American Mineralogist*, **105**, 109–122.

Biagioni C., Sejkora J., Raber T., Roth P., Moëlo Y., Dolníček Z. and Pasero M. (2021) Tennantite-(Hg), $Cu_6(Cu_4Hg_2)As_4S_{13}$, a new tetrahedrite-group mineral from the Lengenbach quarry, Binn, Switzerland. *Mineralogical Magazine*, **85**, 744–751.

Biagioni C., Kasatkin A.V., Sejkora J., Nestola F. and Škoda R. (2022) Tennantite-(Cd), IMA 2021-083. CNMNC Newsletter 65, *Mineralogical Magazine*, **86**, https://doi.org/10.1180/mgm.2022.14

Bosi F., Hatert F., Hålenius U., Pasero M., Miyawaki R. and Mills S.J. (2019) On the application of the IMA-CNMNC dominant-valency rule to complex mineral compositions. *Mineralogical Magazine*, **83**, 627–632.

Brese N.E. and O'Keeffe M. (1991) Bond-valence parameters for solids. *Acta Crystallographica,* **B47**, 192–197.

Bruker AXS Inc. (2016) *APEX 3*. Bruker Advanced X-ray Solutions, Madison, Wisconsin, USA.

Catchpole H., Kouzmanov K. and Fontboté L. (2012) Copper-excess stannoidite and tennantite-tetrahedrite as proxies for hydrothermal fluid evolution in a zoned cordilleran base metal district, Morococha, Central Peru. *The Canadian Mineralogist*, **50**, 719–743.

Cesbron F., Giraud R., Picot P. and Pillard F. (1985) La vinciennite, $Cu_{10}Fe_4Sn(As,Sb)S_{16}$, une nouvelle espèce minérale. Etude paragénétique du gîte type de Chizeuil, Saône-et-Loire. *Bulletin de Minéralogie*, **108**, 447–456.

Charlat M. and Lévy C. (1974) Substitutions multiples dans la série tennantite-tétraédrite. *Bulletin de la Société Française de Mineralogie et de Cristallographie*, **97**, 241–250.

Charlat M. and Lévy C. (1975) Influence des principales substitutions sur le parametre cristallin de la série tennantite-tétraédrite. *Bulletin de la Société Française de Mineralogie et de Cristallographie*, **98**, 152–158.

Charnock J.M., Garner C.D., Pattrick R.A.D. and Vaughan D.J. (1989) EXAFS and Mössbauer spectroscopic study of Fe-bearing tetrahedrites. *Mineralogical Magazine*, **53**, 193–199.

Chetty R., Bali A. and Mallik R.C. (2015) Tetrahedrites as thermoelectric materials: an overview. *Journal of Material Chemistry C*, **3**, 12364–12378.

Criddle A.J. and Stanley C.J. (1993) *Quantitative data file for ore minerals*, *3rd edition*. Chapman & Hall, London.

Des Cloizeaux M. (1855) Notices Minéralogiques. Sur les formes cristallines de la Dufrénoysite. *Annales des Mines*, **5**, 389–398.

Di Benedetto F., Bernardini G.P., Cipriani C., Emiliani C., Gatteschi D. and Romanelli M. (2005) The distribution of Cu(II) and the magnetic properties of the synthetic analogue of tetrahedrite: $Cu_{12}Sb_4S_{13}$. *Physics and Chemistry of Minerals*, **32**, 155–164.

Flack H.D. (1983) On enantiomorph-polarity estimation. *Acta Crystallographica,* **A39**, 876–881.

Gainov R.R., Dooglav A.V., Pn'kov I.N., Mukamedshin I.R., Savinkov A.V. and Mozgova N.N. (2008) Copper valence, structural separation and lattice dynamics in tennantite: NMR, NQR and SQUID studies. *Physics and Chemistry of Minerals*, **35**, 37–48.

Hathwar V.R., Nakamura A., Kasai H., Suekuni K., Tanaka H.I., Takabatake T., Iversen B.B. and Nishibori E. (2019) Low-Temperature Structural Phase Transitions in Thermoelectric Tetrahedrite, $Cu_{12}Sb_4S_{13}$, and Tennantite, $Cu_{12}As_4S_{13}$. *Crystal Growth & Design*, **19**, 3979–3988.

Johan Z. and Le Bel L. (1980) Minéralogie des minéralisations type porphyre cuprifère rencontrées dans les batholites de la Caldera et de Colombie Britannique. *Mémoire BRGM*, **99**, 141–149.

Johnson M.L. and Burnham C.W. (1985) Crystal structure refinement of an arsenic-bearing argentian tetrahedrite. *American Mineralogist*, **70**, 165–170.

Johnson N.E., Craig J.R. and Rimstidt J.D. (1986) Compositional trends in tetrahedrite. *The Canadian Mineralogist*, **24**, 385–397.

Johnson N.E., Craig J.R. and Rimstidt J.D. (1987) Effect of substitutions on the cell dimensions of tetrahedrite. *The Canadian Mineralogist*, **25**, 237–244.

Johnson N.E., Craig J.R. and Rimstidt J.D. (1988) Crystal chemistry of tetrahedrite. *American Mineralogist*, **73**, 389–397.

Kouzmanov K., Ramboz C., Bailly L. and Bogdanov K. (2004) Genesis of high-sulfidation vinciennite-bearing Cu–As–Sn (±Au) assemblage from the Radka epithermal copper deposit, Bulgaria: evidence from mineralogy, and infrared microthermometry of enargite. *The Canadian Mineralogist*, **42**, 1501–1521.

Kraus W. and Nolze G. (1996) POWDER CELL – a program for the representation and manipulation of crystal structures and calculation of the resulting X-ray powder patterns. *Journal of Applied Crystallography*, **29**, 301–303.

Levinsky P., Candolfi C., Dauscher A., Tobola A., Hejtmánek J. and Lenoir B. (2019) Thermoelectric properties of the tetrahedrite–tennantite solid solutions $Cu_{12}Sb_{4-x}As_xS_{13}$ and $Cu_{10}Co_2Sb_{4-y}As_yS_{13}$ ($0 \le x,y \le 4$). *Physical Chemistry Chemical Physics*, **21**, 4547–4555.

Lind I.L. and Makovicky E. (1982) Phase relations in the system Cu–Sb–S at 200°C, 108 Pa by hydrothermal synthesis. Microprobe analyses of tetrahedrite – a warning. *Neues Jahrbuch für Mineralogie, Abhandlungen*, **145**, 134–156.

Lu X. and Morelli D.T. (2013) Natural mineral tetrahedrite as a direct source of thermoelectric materials. *Physical Chemistry Chemical Physics*, **15**, 5762–5766.

Makovicky E., Forcher K., Lottermoser W. and Amthauer G. (1990) The role of Fe^{2+} and Fe^{3+} in synthetic Fe-substituted tetrahedrite. *Mineralogy and Petrology*, **43**, 73–91.

Makovicky E., Tippelt G., Forcher K., Lottermoser W., Karup-Møller S. and Amthauer G. (2003) Mössbauer study of Fe-bearing synthetic tennantite. *The Canadian Mineralogist*, **41**, 1125–1134.

Makovicky E., Karanović L., Poleti D., Balić-Žunić T. and Paar W.H. (2005) Crystal structure of copper-rich unsubstituted tennantite, $Cu_{12.5}As_4S_{13}$. *The Canadian Mineralogist*, **43**, 679–688.

Marcoux E., Moëlo Y. and Milési J.P. (1994) Vinciennite and Cu-excess tennantite from the Layo (Cu,Sn,As,Au) epithermal deposit (Southern Peru). *Mineralogy and Petrology*, **51**, 21–36.

Maske S. and Skinner B.J. (1971) Studies of the sulfosalts of copper. I. Phases and phase relations in the system Cu–As–S. *Economic Geology*, **66**, 901–918.

Morozewicz J. (1926) Trois minéraux polonais. *Congrés Géologique International, Comptes Rendus de la XIIIE Session, en Belgique* 1922, **3**, 1619–1621.

Nasonova D.I., Presniakov I.A., Sobolev A.V., Verchenko V.Yu., Tsirlin A.A., Wei Z., Dikarev E.V. and Shevelkov A.V. (2016) Role of iron in synthetic tetrahedrites revisited. *Journal of Solid State Chemistry*, **242**, 62–69.

Pattrick R.A.D., van der Laan G., Vaughan D.J. and Henderson C.M.B. (1993) Oxidation state and electronic configuration determination of copper in tetrahedrite group minerals by *L*-edge X-ray absorption spectroscopy. *Physics and Chemistry of Minerals*, **20**, 395–401.

Phillips R. (1819) Analysis of the copper ore, described in the preceding paper. *The Quarterly Journal of Science, Literature and the Arts*, **7**, 100–102.

Phillips W. (1819) Description of an ore of copper from Cornwall. *The Quarterly Journal of Science, Literature and the Arts*, **7**, 95–100.

Plattner C.F. (1846) Chemische Analyse der Kuperblende. *Annalen der Physik und Chemie*, **143**, 422–423.

Pouchou J.L., and Pichoir F. (1985) "PAP" (φρZ) procedure for improved quantitative microanalysis. Pp. 104–106 in: *Microbeam Analysis* (J.T. Armstrong, editor). San Francisco Press, San Francisco.

Repstock A., Voudouris P. and Kolitsch U. (2015) New occurrences of watanabeite, colusite, "arsenosulvanite", and "Cu-excess" tetrahedrite-tennantite at the Pefka high-sulfidation epithermal deposit, northeastern Greece. *Neues Jahrbuch für Mineralogie, Abhandlungen*, **192**, 135–149.

Sejkora J., Biagioni C., Vrtiška L. and Moëlo Y. (2021) Zvěstovite-(Zn), $Ag_6(Ag_4Zn_2)As_4S_{13}$, a new tetrahedrite-group mineral from Zvěstov, Czech Republic. *Mineralogical Magazine*, **85**, 716–724.

Sheldrick G.M. (2015) Crystal Structure Refinement with SHELXL. *Acta Crystallographica*, **C71**, 3–8.

Sobolev A.V., Presniakov I.A., Nasonova D.I., Verchenko V.Yu. and Shevelkov A.V. (2017) Thermally activated electron exchange in $Cu_{12-x}Fe_xSb_4S_{13}$ (x = 1.3, 1.5) tetrahedrites: A Mössbauer study. *Journal of Physical Chemistry*, **121**, 4548–4557.

Thouvenin J.M. (1983) *Les Minéralisations Polymétalliques à Pb–Zn–Cu–Ag de Huaron (Pérou Central)*. Thesis, ENSM, Paris, 210 pp.

Velebil D., Hyršl J., Sejkora J. and Dolníček Z. (2021) Chemistry and classification of of minerals of tetrahedrite group from deposits of Peru. *Bulletin Mineralogie Petrologie*, **29**, 321–336 [in Czech].

Voudouris P., Repstock A., Spry P.G., Frenzel M., Mavrogonatos C., Keith M., Tarantola A., Melfos V., Tombros S., Zhai D., Cook N.J., Ciobanu C., Schaarschmidt A., Rieck B., Kolitsch U. and Falkenberg J.J. (2022) Physicochemical constraints on indium-, tin-, germanium-, gallium-, gold-, and tellurium-bearing mineralizations in the Pefka and St Philippos polymetallic vein- and breccia-type deposits, Greece. *Ore Geology Reviews*, **140**, 104348.

Wang Y., Chen R., Gu X., Hou Z., Yang Z., Dong G., Guo H. and Qu K. (2021) Tetrahedrite-(Ni), IMA 2021-031. CNMNC Newsletter 62. *Mineralogical Magazine*, **85**, 634–638, https://doi.org/10.1180/mgm.2021.62

Warr L.N. (2021) IMA-CNMNC approved mineral symbols. *Mineralogical Magazine*, **85**, 291–320.

Welch M.D., Stanley C.J., Spratt J. and Mills S.J. (2018) Rozhdestvenskayaite $Ag_{10}Zn_2Sb_4S_{13}$ and argentotetrahedrite $Ag_6Cu_4(Fe^{2+},Zn)_2Sb_4S_{13}$: two Ag-dominant members of the tetrahedrite group. *European Journal of Mineralogy*, **30**, 1163–1172.

Wilson A.J.C. (1992) *International Tables for Crystallography*. Volume C. Kluwer, Dordrecht, The Netherlands.

Wuensch B.J. (1964) The crystal structure of tetrahedrite, $Cu_{12}Sb_4S_{13}$. *Zeitschrift für Kristallographie*, **119**, 437–453.

Wuensch B.J., Takéuchi Y. and Nowacki W. (1966) Refinement of the crystal structure of binnite, $Cu_{12}As_4S_{13}$. *Zeitschrift für Kristallographie*, **123**, 1–20.

Yaroslavzev A.A., Kuznetsov A.N., Dudka A.P., Mironov A.V., Buga S.G. and Denisov V.V. (2021) Laves polyhedra in synthetic tennantite, $Cu_{12}As_4S_{13}$, and its lattice dynamics. *Journal of Solid State Chemistry*, **297**, 122061.

https://doi.org/10.1180/mgm.2022.26 Published online by Cambridge University Press